Piezoelectric and dielectric properties of Pb(Zr,Ti)O_{3} ferroelectric bilayers

Alexei Grigoriev, Chun Yang, Mandana Meisami Azad, Oliver Causey, Donald A. Walko, Daniel S. Tinberg, and Susan Trolier-McKinstry

Phys. Rev. B **91**, 104106 — Published 9 March 2015

DOI: 10.1103/PhysRevB.91.104106

Piezoelectric and dielectric properties of $Pb(Zr,Ti)O_3$ ferroelectric bilayers

Alexei Grigoriev,[1,*] Chun Yang,[1] Mandana Meisami Azad,[1] Oliver Causey,[1] Donald A. Walko,[2] Daniel S. Tinberg,[3] and Susan Trolier-McKinstry [3]

[1] Department of Physics and Engineering Physics, The University of Tulsa, Tulsa, OK 74104, USA

[2] Advanced Photon Source, Argonne National Laboratory, Argonne, IL 60439, USA

[3] Department of Materials Science and Engineering, Pennsylvania State University, University Park, PA 16802, USA

The dielectric and piezoelectric properties of an epitaxial $PbZr_{0.8}Ti_{0.2}O_3/PbZr_{0.6}Ti_{0.4}O_3$ ferroelectric bilayer film were studied. Time-resolved synchrotron x-ray microdiffraction provided access to layer-specific structural information during electric-field induced changes. The observed dielectric and electro-mechanical responses are consistent with a weak electrostatic polarization coupling and can be described using a thermodynamic model of epitaxial ferroelectric bilayers. The weak electrostatic coupling between ferroelectric layers can enable unusual tail-to-tail and head-to-head polarization configurations. X-ray measurements of the piezoelectric response of the ferroelectric bilayer at a microsecond time scale confirmed a possible tail-to-tail polarization domain configuration.

* Author to whom correspondence should be addressed: alexei-grigoriev@utulsa.edu

INTRODUCTION

Recent theoretical efforts to describe properties of ferroelectric multilayers suggested that the dielectric and piezoelectric responses can be controlled by varying the strain and volume fraction of each of the ferroelectric layers.[1-3] Epitaxial strain and electrostatic polarization coupling between ferroelectric layers can lead to the enhancements of the dielectric permittivity and piezoelectric coefficients. Multilayer materials with engineered ferroelectric properties are of particular interest because of their applications in tunable dielectric devices and electromechanical sensors and actuators.[3-5] A simple electrostatic coupling model for an ideal ferroelectric bilayer predicts strong depolarizing fields which act to reduce the electric polarization gradient across the interface.[6] This model predicts almost constant electric polarization throughout all layers of an ideally coupled ferroelectric multilayer system.[7, 8] Such uniform electric polarization has been reported for thin film superlattices. For instance, x-ray measurements of electro-mechanical response of a complex oxide $CaTiO_3/BaTiO_3$ superlattice showed a continuous electric polarization throughout the multilayer structure.[7] Any deviation from this behavior for an ideally coupled system will increase with increasing thickness of the ferroelectric layers due to the screening of the induced depolarizing fields and due to structural and electrostatic imperfections. For example, the electric polarization can be different at the interface and in the bulk of an epitaxial ferroelectric film due to structural relaxation effects.[9, 10].

Ferroelectric and dielectric properties can be very different in thick layers and in ultra-thin films because of the thickness dependence of structural relaxation and interfacial space charge effects.[9-11] It is interesting to test the uniformity of polarization in ferroelectric multilayers of an intermediate thickness of tens to hundreds of nanometers. If the electric polarization gradient is compensated by charges at a ferroelectric/ferroelectric interface,

decoupling should result in the stable configuration of tail-to-tail or head-to-head domains.[12] This article discusses polarization coupling and dielectric properties of a $Pb(Zr,Ti)O_3$ bilayer of 100-nm thick ferroelectric layers.

EXPERIMENTAL DETAILS AND THEORY

Advances in epitaxial growth of thin films and structural characterization techniques provide new opportunities to synthesize complex oxide multilayers and probe electric-field induced changes in the crystal structure of individual layers of the thin-layer systems.[7, 13-17] This work explores the properties of the ferroelectric bilayer that consists of $PbZr_xTi_{1-x}O_3$ (PZT) layers of two different chemical compositions (80/20 at x=0.8, and 60/40 at x=0.6) epitaxially grown on top of the $SrRuO_3/SrTiO_3$ [001] substrate using pulsed-laser deposition.[18] The thicknesses of the top and bottom ferroelectric layers were approximately 120 nm and 95 nm, respectively, while the $SrRuO_3$ bottom electrode was 90 nm. An array of 40 nm thick polycrystalline platinum top electrodes was prepared using lift-off processing. Dielectric and time-resolved structural measurements were conducted on ferroelectric capacitors with top electrode diameters of 200 μm and 150 μm. Time-resolved x-ray microdiffraction probed the electric-field dependent crystal structure of ferroelectric capacitors using 10 keV synchrotron x-ray radiation at sector 7 of the Advanced Photon Source (APS) at the Argonne National Laboratory. X rays were focused to the spot size of approximately 20×20 μm^2 using Kirkpatrick-Baez mirror optics. The x-ray beam remained entirely on a 200-μm diameter ferroelectric capacitor during diffraction measurements. The x-ray diffraction setup was compatible with an electrical probe station enabling diffraction experiments that were synchronized with electrical signals applied to ferroelectric capacitors. Previous experiments at

the APS used a similar setup for probing polarization and strain dynamics in single-layer ferroelectric thin films.[19, 20] Dielectric properties of ferroelectric bilayers were studied by analyzing the response of the capacitors to mixed dc+ac signals. This approach, which is described elsewhere,[21] uses a long-memory-depth digital oscilloscope (LeCroy WavePro 725Zi, 2.5 GHz bandwidth) to collect dielectric response data.

The Landau-Ginzburg-Devonshire thermodynamic theory of ferroelectrics can predict equilibrium properties, including the spontaneous polarization and dielectric permittivity, of single-phase ferroelectric systems at given values of temperature and strain.[22-24] As described by Pertsev et al., the Gibbs free energy of an epitaxially strained PZT film is given by:[23]

$$\begin{aligned} G = {} & \frac{s_m^2}{s_{11}+s_{12}} + 2a_1^* P_{xy}^2 + a_3^* P_z^2 + \left(2a_{11}^* + a_{12}^*\right) P_{xy}^4 + 2a_{13}^* P_{xy}^2 P_z^2 + a_{33}^* P_z^4 \\ & + a_{111}\left(2P_{xy}^6 + P_z^6\right) + 2a_{112}\left(P_{xy}^6 + P_{xy}^4 P_z^2 + P_{xy}^2 P_z^4\right) + a_{123} P_{xy}^4 P_z^2 - P_z E_z \end{aligned} \tag{1}$$

where a_i^*, a_{ij}^*, a_i, a_{ij}, and a_{ijk} are the stiffness coefficients, s_m is the misfit strain, s_{ij} are elastic compliances, and E_z is the external electric field component in the surface normal direction. P_{xy} and P_z are the electric polarizations in the in-plane and in the surface normal directions. It is assumed here that $P_x = P_y = P_{xy}$ and that the electric field is applied along the *z*-direction only. Using available data for stiffness coefficients and elastic compliances, minimization of the Gibbs free energy (1) provides equilibrium polarization values for a PZT film of any composition at given temperature and misfit strain.[23, 25] The relative dielectric permittivity can be calculated by finding the derivative of polarization with respect to electric field:

$$\varepsilon_z^r = 1 + \frac{1}{\varepsilon_0}\left.\frac{\partial P_z}{\partial E_z}\right|_{E_z=0}, \tag{2}$$

where ε_0 is the permittivity of free space.

This thermodynamic approach can be extended to electrostatically coupled ferroelectric bilayers:[1, 26]

$$G_{bilayer} = (1-\alpha) G_1 + \alpha G_2 + \frac{\alpha(1-\alpha)\xi'}{2\varepsilon_0 \varepsilon_b} (P_{z1} - P_{z2})^2, \quad (3)$$

where α is the relative volume fraction of layer 2, ξ' is the electrostatic coupling coefficient, and ε_b is the background dielectric permittivity. The background dielectric permittivity can be important to describe ferroelectric systems.[27-30] However, the effect of the background permittivity in this work is limited to the scaling of the coupling coefficient because the typical values of the background dielectric permittivity of ~7 are small relative to the dielectric permittivity of perovskite ferroelectrics, and the background permittivity is expected to be approximately the same in both PZT layers.[28, 31] We will redefine $\xi = \xi'/\varepsilon_b$ as the electrostatic coupling coefficient for simplicity of discussion. The electrostatic coupling strength ξ for a bilayer with a fixed volume fraction α can be analyzed using equation (3). If the coupling coefficient is 0, the layers act as independent ferroelectric layers, while if the coupling coefficient is 1, the layers are completely coupled. The effects of electrostatic coupling on the properties of bilayers include the polarization gradient reduction at the interface between the layers and depolarizing electric fields that affect the stability and switching of polarization domains. If the coupling is weak, the electric polarization in each ferroelectric layer can be switched independently.

Obtaining the equilibrium values of the electric polarizations of a PZT bilayer requires four-dimensional minimization of the free energy in equation (3) using in-plane, P_{xy1} and P_{xy2},

and out-of-plane, P_{z1} and P_{z2}, polarizations as independent parameters. The average dielectric permittivity of the bilayer and piezoelectric coefficients d_{33} of ferroelectric layers can be found from:

$$\varepsilon^r_{z,bilayer} = \frac{\varepsilon^r_{z,1}\varepsilon^r_{z,2}}{\left[(1-\alpha)\varepsilon^r_{z,2} + \alpha\varepsilon^r_{z,1}\right]} \tag{4}$$

$$d_{33} = 2P_z\varepsilon_0\left(\varepsilon^r_z - 1\right)\left(Q_{11} - \frac{2s_{12}Q_{12}}{s_{11}+s_{12}}\right), \tag{5}$$

where Q_{ij} are electrostrictive coefficients. The relative dielectric permittivities in equations (4) and (5) are calculated here in the presence of internal depolarizing fields in coupled ferroelectric layers. The results of such calculations can then be compared with experimental results of dielectric and piezoelectric measurements in order to analyze the interlayer coupling strength ξ.

RESULTS AND DISCUSSION

In order to test the strength of electrostatic polarization coupling in ferroelectric bilayers, the piezoelectric strain in each layer can be probed by time-resolved x-ray microdiffraction. This technique is sensitive to the changes in lattice parameters of the individual layers during the application of an electric field.[7, 19, 32] Fig. 1 shows a $\theta-2\theta$ x-ray diffraction scan along the specular [001] crystallographic direction. This scan includes the PZT (002) Bragg peaks of both 80/20 and 60/40 ferroelectric layers. The fact that the Bragg peaks of the ferroelectric layers are easily resolved in diffraction scans can be used to test the response of each layer to an applied electric field. The two scans shown in Fig. 1 were taken before and during the application of 500 kV/cm electric field. The Bragg peaks in the scan that was measured under the applied electric

field are shifted to lower scattering angles. These shifted peaks indicate the expansion of the crystal lattice in the surface normal direction. Piezoelectric strain $s_z = (c - c_0)/c_0$, where c and c_0 are the surface normal lattice parameters at an applied field and at a zero field, respectively, can readily be obtained from the electric-field induced changes in the Bragg peak position.[33]

The piezoelectric strain as a function of the applied voltage is shown in Fig. 2 for PZT 80/20 and PZT 60/40 layers. These measurements were done using triangular bipolar voltage pulses at the frequency of 100 Hz. The amplitude of the voltage signals of ±10 V was several times greater than the low-frequency polarization switching voltage of ±3 V, observed in ferroelectric hysteresis measurements at 2.5 kHz (100 μs 0-to-10 V rise time) frequency (Fig. 3). It is reasonable to expect that polarization switching is completed before the applied voltage reaches its maximum value of 10 V at 100 Hz signal frequency. The disappearance of hysteresis at high voltage magnitudes (>8 V and <-8 V) supports this expectation. However, the changes of the piezoelectric strain with voltage, and hence d_{33} piezoelectric coefficients, are different at lower voltage magnitudes. The d_{33} piezoelectric coefficients depend on the voltage sweep direction. The hysteresis in piezoelectric strain is the strongest for the bottom PZT 60/40 layer at $P_z < 0$ (positive applied voltage with respect to a grounded bottom electrode) and for the top PZT 80/20 layer at $P_z > 0$ (negative applied voltage). A negative charge accumulating at the interface between ferroelectric layers or positive charges accumulating at the electrode/ferroelectric interfaces and then dissipating at higher applied voltages can explain the observed nonlinearities in piezoelectric response.

The importance of the effects of charge motion on ferroelectric properties of the bilayer is further supported by a strong coercive field dependence on the voltage ramp rate (Fig. 3). The

mobile charges in ferroelectric layers should reduce the strength of the electrostatic coupling because the coupling coefficient in (3) depends on the ratio of bound and free charge densities as $\xi = 1 - \left(\rho_{free} / \rho_{bound} \right)$.[6, 26] In order to provide a quantitative argument to verify the weak electrostatic coupling, the results of thermodynamic calculations can be compared with experimentally obtained values of the d_{33} piezoelectric coefficient and dielectric permittivity of the bilayer.

Maps in Fig. 4 show the changes in the average relative dielectric permittivity of the bilayer (Fig. 4(a)) and in the d_{33} piezoelectric coefficients of the top (Fig. 4(c)) and bottom (Fig. 4(d)) layers with epitaxial strain and coupling strength. In these calculations, the same values of epitaxial strain were used for both ferroelectric layers, and the volume fraction was fixed at $\alpha = 95/(120+95) = 0.442$. The maps show that the dielectric and piezoelectric properties are enhanced at the phase boundaries; this information can be useful for synthesizing new ferroelectric materials with enhanced dielectric permittivity and piezoelectric response. The range of epitaxial strains that is relevant to the PZT bilayer under investigation in this work is near $s_m = 0$ because PZT films thicker than 100 nm are expected to be relaxed.[34] At small values of misfit strain, the relative dielectric permittivity of the bilayer changes monotonically at low values of $\varepsilon^r_{theory} = 235$ at $s_m = -0.002$ and $\varepsilon^r_{theory} = 260$ at $s_m = 0$. The strength of the polarization coupling has almost no effect on the permittivity in this range of strains. The experimentally obtained average dielectric permittivity[21] $\varepsilon^r_{\exp} = 261$ is very close to the permittivity predicted for a completely relaxed bilayer. The changes in the d_{33} piezoelectric coefficients as a function of the coupling strength are shown in Fig. 4(b) for a special case of zero epitaxial strain. In this case, the calculated d_{33} piezoelectric coefficients of uncoupled (

$\xi = 0$) PZT 60/40 and 80/20 layers are 72 pm/V and 47 pm/V, respectively, whereas they are 62 pm/V and 52 pm/V for strongly coupled layers ($\xi = 1$). These calculations show that the difference between piezoelectric coefficients of ferroelectric layers depends on the coupling strength. This can be used to analyze the coupling by comparing experimentally measured and calculated piezoelectric coefficients. The average piezoelectric coefficients of the layers can be derived from data in Fig. 2. At strong electric fields, where the hysteresis in piezoelectric response is small, these coefficients are approximately 110 pm/V and 55 pm/V, for PZT 60/40 and 80/20 layers, respectively. The large difference between the measured piezoelectric coefficients of the layers are better explained by the model with the weak electrostatic coupling.

Weak coupling between ferroelectric layers creates the possibility of independent manipulation of the electric polarization in each layer. Practically, it can be challenging to switch the polarization in one layer without switching it in the second one, even for ideally decoupled layers, unless the switching voltages are significantly different for the two ferroelectric materials and there is a sufficient time to compensate the switching charge at the ferroelectric/ferroelectric interface.[35] In particular, the charged domain walls that should form as a result of head-to-head or tail-to-tail domain configurations, can partially compensate the switching charge.[36]. Multiple switching thresholds that would indicate independent polarization switching of the layers were not detected in hysteresis loop measurements (Fig. 3). It might be possible, however, to switch the polarization of only one of the ferroelectric layers of the bilayer by applying short electric field pulses instead of a continuously changing signal, provided the polarization dynamics are different for the two layers.

To begin to address this point, the piezoelectric response of the bilayer was measured during the application of 5-μs square pulses. The pulse voltage was cycled several times

between -10 V and +10 V in steps of 0.1 V. It is expected that the piezoelectric strains of ferroelectric layers with a parallel polarization alignment will have the same signs, and the strains of the layers with an antiparallel polarization alignment will have opposite signs. It was found that different signs of the piezoelectric strains were observed for the two ferroelectric layers in the time-resolved x-ray microdiffraction scans for short voltage pulses between +4 V and +5 V. The x-ray diffraction scans in Fig. 5 show the (002) Bragg peaks of the layers before and during application of +4.5 V 5-μs voltage pulses. The peak of the bottom PZT 60/40 layer is shifted to a smaller scattering angle, which corresponds to a tensile piezoelectric strain. The peak of the top PZT 80/20 layer is shifted in the opposite direction, corresponding to a compressive piezoelectric strain. This data strongly suggest that the electric polarizations are antiparallel in the two ferroelectric layers forming a tail-to-tail domain configuration. There should be a mechanism by which the switching charge is compensated at the interface between the ferroelectric layers. The charge compensation requirement could be satisfied by an increase of the charge carrier concentration at the charged tail-to-tail PZT/PZT domain wall if the carrier concentration at the PZT domain walls is enhanced similar to the charge carrier density enhancement reported for $BaTiO_3$ tail-to-tail and head-to-head domain walls.[36] If the PZT film acts as a *p*-type semiconductor,[37] then charge compensation should be easier for tail-to-tail domain walls than head-to-head domain walls. This is consistent with the observation of only tail-to-tail domain walls in the PZT/PZT bilayer. A charged domain wall can form even for a tail-to-head configuration of PZT layers of different compositions. If the charge carrier concentration at the domain wall is enhanced, the electrostatic coupling between ferroelectric layers should be weakened. The electronic structure properties of the charged PZT/PZT domain walls can be an interesting topic for further theoretical and experimental research.

CONCLUSIONS

It was found that the coupling between ~100-nm PZT ferroelectric layers is significantly weaker than the coupling observed in superlattices.[7] The experimentally observed difference between d_{33} piezoelectric coefficients of individual ferroelectric layers is significantly larger than the difference predicted for ideally coupled layers. The asymmetry in the observed piezoelectric response of the layers indicates the presence of internal electric fields that can be created by electric charges accumulating at the interfaces. The diffraction data are consistent with the formation of charged domain walls between the ferroelectric layers. The weak electrostatic coupling provides an opportunity for manipulation of the polarization state in individual ferroelectric layers. An antiparallel tail-to-tail orientation of the electric polarization in ferroelectric layers was confirmed by time-resolved x-ray microdiffraction using 5-μs voltage pulses. This tail-to-tail polarization domain configuration is similar to the configuration predicted for a hypothetical multidomain system in which ferroelectric domains are separated by layers of donors and acceptors.[12] If the carrier density enhancement at the charged PZT/PZT domain wall is similar to the enhancement predicted for $BaTiO_3$,[36] the domain wall can be responsible for the switched charge compensation and for the weak interlayer coupling.

ACKNOWLEDGEMENTS

This work was supported by the NSF DMR (award No. DMR-1057159). The use of the Advanced Photon Source was supported by the U. S. Department of Energy, Office of Science, Office of Basic Energy Sciences, under Contract No. DE-AC02-06CH11357.

[1] M. B. Okatan, J. V. Mantese, and S. P. Alpay, Phys. Rev. B **79**, 174113 (2009).

[2] V. R. Cooper and K. M. Rabe, Phys. Rev. B **79**, 180101 (2009).

[3] R. Mahjoub, S. P. Alpay, and V. Nagarajan, Phys. Rev. Lett. **105**, 197601 (2010).

[4] R. Nath, S. Zhong, S. P. Alpay, B. D. Huey, and M. W. Cole, Appl. Phys. Lett. **92**, 012916 (2008).

[5] M. B. Okatan, M. W. Cole, and S. P. Alpay, J. Appl. Phys. **104** (2008).

[6] J. V. Mantese and S. P. Alpay, *Graded Ferroelectrics, Transcapacitors and Transponents* (Springer Science+Business Media, Inc., New York, 2005).

[7] J. Y. Jo, R. J. Sichel, H. N. Lee, S. M. Nakhmanson, E. M. Dufresne, and P. G. Evans, Phys. Rev. Lett. **104**, 207601 (2010).

[8] M. Dawber, C. Lichtensteiger, M. Cantoni, M. Veithen, P. Ghosez, K. Johnston, K. M. Rabe, and J. M. Triscone, Phys. Rev. Lett. **95**, 177601 (2005).

[9] B. S. Kwak, A. Erbil, B. J. Wilkens, J. D. Budai, M. F. Chisholm, and L. A. Boatner, Phys. Rev. Lett. **68**, 3733 (1992).

[10] C. L. Jia, V. Nagarajan, J. Q. He, L. Houben, T. Zhao, R. Ramesh, K. Urban, and R. Waser, Nat. Mater. **6**, 64 (2007).

[11] I. B. Misirlioglu, M. Alexe, L. Pintilie, and D. Hesse, Appl. Phys. Lett. **91**, 022911 (2007).

[12] X. Wu and D. Vanderbilt, Phys. Rev. B **73**, 020103 (2006).

[13] H. N. Lee, H. M. Christen, M. F. Chisholm, C. M. Rouleau, and D. H. Lowndes, Nature **433**, 395 (2005).

[14] A. Grigoriev, D. H. Do, P. G. Evans, B. Adams, E. Landahl, and E. M. Dufresne, Rev. Sci. Instrum. **78**, 023105 (2007).

[15] A. Grigoriev, D. H. Do, D. M. Kim, C. B. Eom, B. Adams, E. M. Dufresne, and P. G. Evans, Phys. Rev. Lett. **96**, 187601 (2006).

[16] E. Bousquet, M. Dawber, N. Stucki, C. Lichtensteiger, P. Hermet, S. Gariglio, J. M. Triscone, and P. Ghosez, Nature **452**, 732 (2008).

[17] P. Chen, M. P. Cosgriff, Q. Zhang, S. J. Callori, B. W. Adams, E. M. Dufresne, M. Dawber, and P. G. Evans, Phys. Rev. Lett. **110**, 047601 (2013).

[18] V. Bornand and S. Trolier-Mckinstry, Thin Solid Films **370**, 70 (2000).

[19] A. Grigoriev, D. Dal-Hyun, P. G. Evans, B. Adams, E. Landahl, and E. M. Dufresne, Rev. Sci. Instrum. **78**, 23105 (2007).

[20] A. Grigoriev, R. J. Sichel, J. Y. Jo, S. Choudhury, L. Q. Chen, H. N. Lee, E. C. Landahl, B. W. Adams, E. M. Dufresne, and P. G. Evans, Phys. Rev. B **80**, 014110 (2009).

[21] P. Salev, M. Meisami-Azad, and A. Grigoriev, J. of Appl. Phys. **113**, 074104 (2013).

[22] S. K. Streiffer, C. Basceri, C. B. Parker, S. E. Lash, and A. I. Kingon, J. Appl. Phys. **86**, 4565 (1999).

[23] N. A. Pertsev, V. G. Kukhar, H. Kohlstedt, and R. Waser, Phys. Rev. B **67**, 054107 (2003).

[24] N. A. Pertsev, A. G. Zembilgotov, and A. K. Tagantsev, Phys. Rev. Lett. **80**, 1988 (1998).

[25] M. J. Haun, Z. Q. Zhuang, E. Furman, S. J. Jang, and L. E. Cross, Ferroelectrics **99**, 45 (1989).

[26] S. Zhong, S. P. Alpay, and J. V. Mantese, Appl. Phys. Lett. **87**, 102902 (2005).

[27] A. Noeth, T. Yamada, A. K. Tagantsev, and N. Setter, J. Appl. Phys. **104**, 094102 (2008).

[28] M. B. Okatan, I. B. Misirlioglu, and S. P. Alpay, Phys. Rev. B **82**, 094115 (2010).

[29] A. K. Tagantsev and G. Gerra, J. Appl. Phys. **100**, 051607 (2006).

[30] A. K. Tagantsev, Ferroelectrics **375**, 19 (2008).

[31] N. Ng, R. Ahluwalia, and D. J. Srolovitz, Phys. Rev. B **86**, 094104 (2012).

[32] A. Grigoriev, R. Sichel, H. N. Lee, E. C. Landahl, B. Adams, E. M. Dufresne, and P. G. Evans, Phys. Rev. Lett. **100**, 027604 (2008).

[33] D. H. Do, A. Grigoriev, D. M. Kim, C. B. Eom, P. G. Evans, and E. M. Dufresne, Integr. Ferroelectr. **101**, 174 (2008).

[34] R. Mahjoub, V. Anbusathaiah, S. P. Alpay, and V. Nagarajan, J. Appl. Phys. **104**, 124103 (2008).

[35] A. Q. Jiang, Y. Y. Lin, and T. A. Tang, Journal of Applied Physics **101**, 104105 (2007).

[36] T. Sluka, A. K. Tagantsev, D. Damjanovic, M. Gureev, and N. Setter, Nat. Commun. **3**, 1751 (2012).

[37] L. Pintilie, M. Lisca, and M. Alexe, J. Optoelectron. Adv. Mater. **8**, 7 (2006).

Figure Captions

FIG. 1. The (002) Bragg peaks of PZT 80/20 (at larger angles) and PZT 60/40 (at smaller angles) at 0 V (black squares) and 10 V (red circles) applied voltages.

FIG. 2. Piezoelectric strain measured at applied voltages from -10 V to +10 V for individual ferroelectric layers of the bilayer capacitor.

FIG. 3. Ferroelectric hysteresis loops measured at three voltage ramp rates: 0.1 $V / \mu s$, 1 $V / \mu s$, and 5 $V / \mu s$.

FIG. 4. Results of thermodynamic calculations of (a) the relative dielectric permittivity and piezoelectric coefficients of (c) the top and (d) bottom layers of the bilayer. *t* and *r* on the maps identify tetragonal and rhombohedral phases, respectively. (b) The dependence of the piezoelectric coefficients of the top and bottom layers on the coupling coefficient at a zero epitaxial strain.

FIG. 5. The (002) Bragg peaks of the ferroelectric layers at 0 V and during application of +4.5 V 5- μs pulses.

Fig. 1

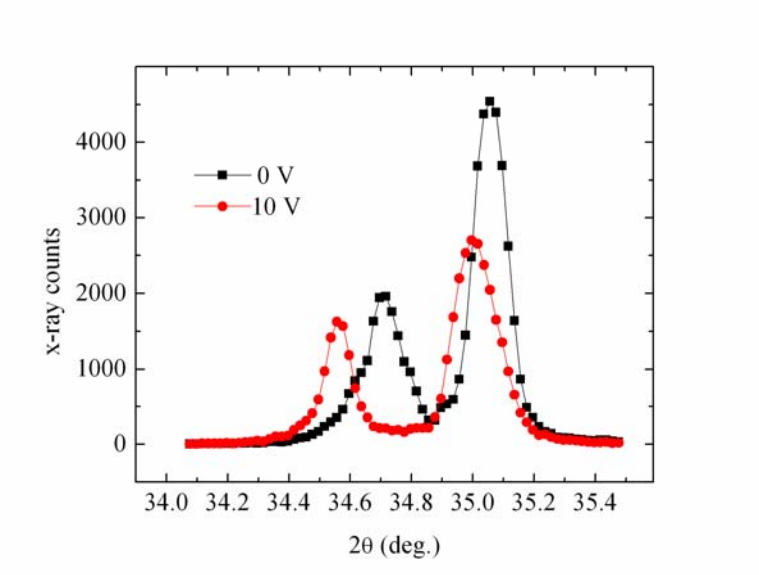
0 V
10 V
x-ray counts
4000
3000
2000
1000
0
34.0
34.2
34.4
34.6
34.8
35.0
35.2
35.4
2θ (deg.)

Fig. 2

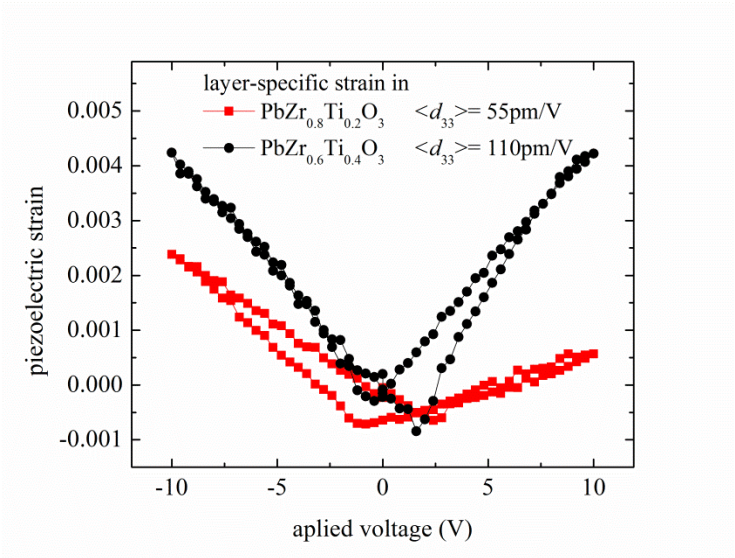
layer-specific strain in
PbZr0.8Ti0.2O3 <d33>= 55pm/V
PbZr0.6Ti0.4O3 <d33>= 110pm/V
piezoelectric strain
0.005
0.004
0.003
0.002
0.001
0.000
-0.001
-10
-5
0
5
10
aplied voltage (V)

Fig. 3

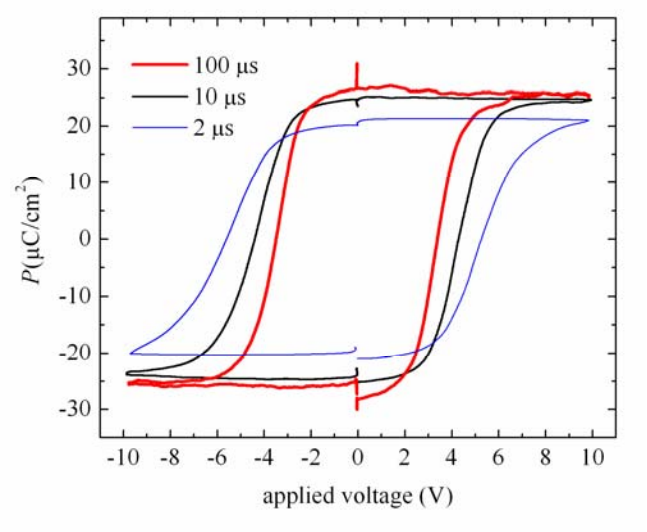
100 μs
10 μs
2 μs
30
20
10
0
-10
-20
-30
P(μC/cm²)
-10 -8 -6 -4 -2 0 2 4 6 8 10
applied voltage (V)

Fig. 4

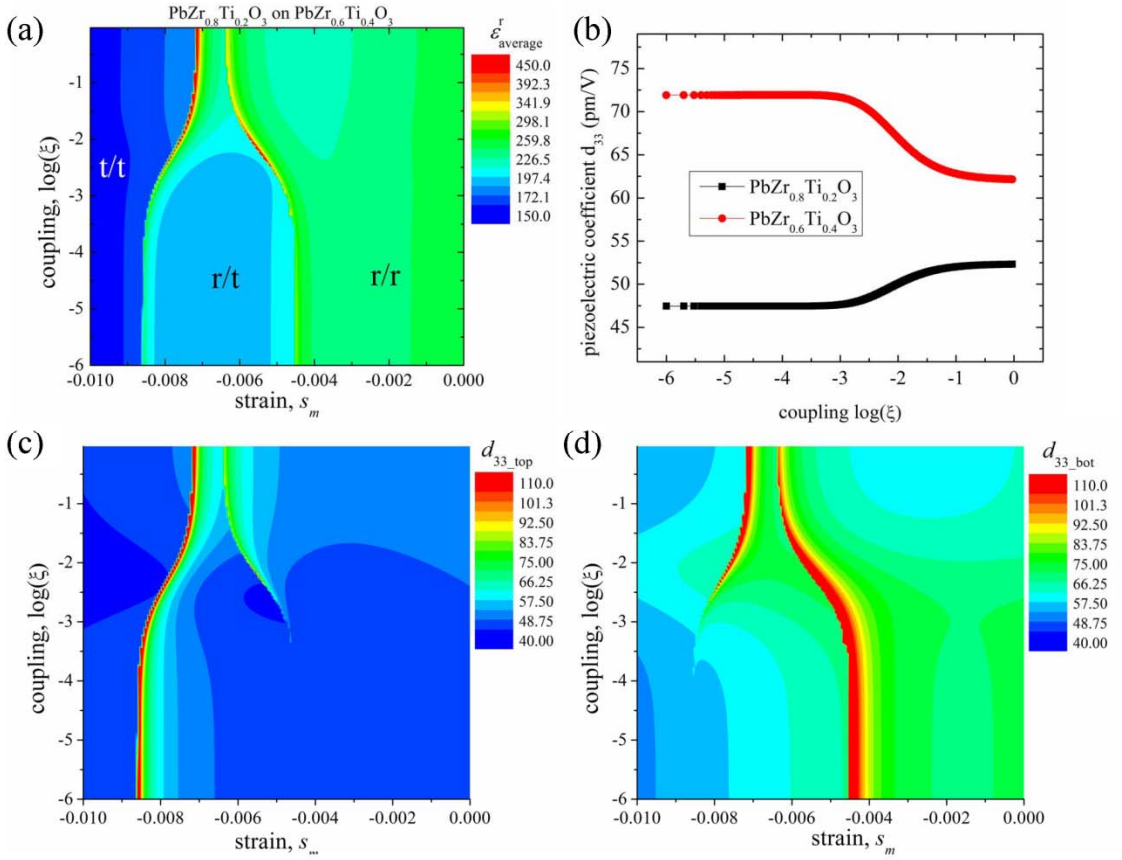
(a)
PbZr0.8Ti0.2O3 on PbZr0.6Ti0.4O3
ε r average
450.0
392.3
341.9
298.1
259.8
226.5
197.4
172.1
150.0
t/t
r/t
r/r
coupling, log(ξ)
strain, sm
(b)
piezoelectric coefficient d33 (pm/V)
PbZr0.8Ti0.2O3
PbZr0.6Ti0.4O3
coupling log(ξ)
(c)
d33_top
110.0
101.3
92.50
83.75
75.00
66.25
57.50
48.75
40.00
coupling, log(ξ)
strain, sm
(d)
d33_bot
110.0
101.3
92.50
83.75
75.00
66.25
57.50
48.75
40.00
coupling, log(ξ)
strain, sm

Fig. 5

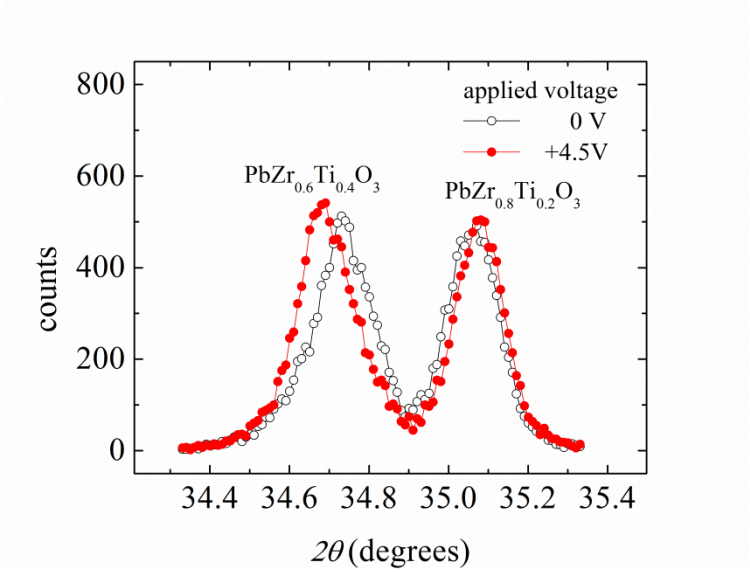
applied voltage
0 V
+4.5V
PbZr0.6Ti0.4O3
PbZr0.8Ti0.2O3
counts
2θ (degrees)